Journal of the Physical Society of Japan
Vol. 52, No. 5, May, 1983, pp. 1814–1824

Study of Frustration Effects in Two-Dimensional Triangular Lattice Antiferromagnets—Neutron Powder Diffraction Study of VX_2, X≡Cl, Br and I

Kinshiro HIRAKAWA, Hiroaki KADOWAKI and Koji UBUKOSHI

Institute for Solid State Physics, University fo Tokyo, Roppongi, Minato-ku, Tokyo

(Received October 15, 1982)

In order to study the frustration effects, we have taken powder diffraction patterns of VX_2 (X≡Cl, Br and I) which are thought to be quasi-two-dimensional triangular lattice antiferromagnets. The spins in VCl_2, VBr_2 and VI_2 were found to order at 36.0, 29.5 and 16.3 K respectively forming a three sublattice structure in the basal plane. Contrary to our expectation, a partially ordered model gives a better fit to the observed diffraction rather than the Néel state with 120° structure though the spins are of Heisenberg symmetry. In VCl_2 and VBr_2, strong diffuse scattering can be observed not only at $T>T_N$ but also at $T\ll T_N$. No critical scattering characteristic for 2D could be seen but the temperature variation of sublattice magnetization is rather close to that for the Ising system.

§1. Introduction

Frustration in spin system is a subject of current interest. One of the typical frustration effect may be seen in the triangular lattice antiferromagnetic system. It is well known that in a triangular lattice antiferromagnet in two-dimension (2D) with n.n. interaction only, no long range order (LRO) occurs at finite temperature if the spins are Ising spin. In the quasi-2D system in which some fraction of XY-nature is contained, a non-collinear Néel structure may appear. However, Fazekas and Anderson[1] have studied a system of $S=1/2$ and argued that for sufficiently lower values of the fraction, the expected ground state is no longer a Néel state but something like a quantum liquid state. Unfortunately, it is scarcely possible to obtain $S=1/2$ triangular lattice antiferromagnet at present. If, however, allowance is given of the entrance of spins greater than one-half, we have several candidates as shown in this paper. We suppose that, some anomalous features, for instance a prominent liquid-like property as for the orientational correlation of spins will appear even in the system with greater spin quantum number.

For the candidates, we consider VX_2 (X≡Cl, Br and I). It is well known that many halides of iron group transition metals crystallize in the CdI_2 structure. In the compounds with more than half filled 3d electrons such as Fe, Co and Ni, the coupling in the plane is ferromagnetic. But, the interplane coupling is antiferromagnetic, the ratio of the coupling constants $|J'/J|$ is, for instance 0.48 in $CoBr_2$[2] showing unexpectedly poor two-dimensionality. In VX_2, on the other hand, the intraplane coupling suggested from the high temperature susceptibility (χ) by Niel *et al.*[3] is strongly antiferromagnetic. The Weiss constants obtained through the χ measurements are 437, 335 and 143 K for VCl_2, VBr_2 and VI_2 respectively. The J values estimated using the series expansion by Rushbrooke and Wood are $J=-23$, -16 and -6 K respectively.[3] Such a strong coupling can not be expected in the interplane coupling, so that in VX_2, we expect better two-dimensionality, though it should be checked by the neutron inelastic scattering. In their χ-T data, no sharp anomalies occur down to 4.2 K except for the sudden drop in χ at 14.5 K in VI_2. All the curves are very flat and no indication of Néel point T_N is found down to 4.2 K. Consequently, we are very much interested in studying VX_2 series by means of neutron scattering technique. It is the purpose of this paper to see the low temperature spin correlation because

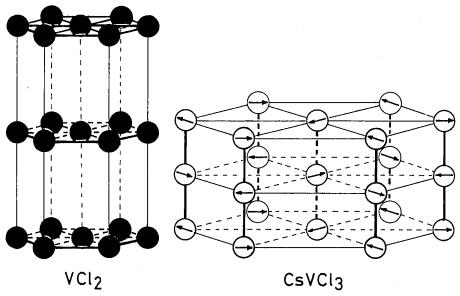

Fig. 1. Comparison of the lattice structures of vanadiun atoms in VCl_2 and $CsVCl_3$. In this figure, the same unit of length is used for the help of comparison.

VX_2 are possibly a good realization of 2D frustrated triangular antiferromagnetic spin system.

Another interesting point of VX_2 is in its relation with $CsVCl_3$ which is an excellent 1D Heisenberg antiferromagnet[3,4] showing striking behaviors. One is the unusually big spin contraction and another is the anomalous temperature dependence of the magnetic Bragg scattering intensity in the 120° structure, i.e. decreasing of the intensity with lowering temperature down to 0.3 K. As supposed by the shortest atomic distance along the *c*-axis in $CsVCl_3$ in Fig. 1, the strongest magnetic interaction is realized in this direction. The interchain distance is much greater and the interaction in the basal plane is weakly antiferromagnetic forming a 120° structure at $T<13.3$ K.[4] The $|J'/J|$ deduced from the recent spin wave measurements[5] is 2.7×10^{-4}. On the other hand, VX_2 are of the layer structure, and the coupling along the *c*-axis is supposedly much weaker than the intraplane coupling. Thus, in $CsVCl_3$ and VX_2, though the electronic structures of V^{2+} are very much the same, but the former is 1D while the latter is 2D. Thus, comparison of the magnetic properties of both is useful to understand the striking properties mentioned above.

As it is difficult to produce big single crystal of VX_2 at present, we shall report a preliminary study on the powdered samples. Growth of bigger crystal is now in progress.

§2. Experimental

Small flaky crystals of VCl_2 are produced by passing HCl gas through the red heated vanadium metal flakes placed in the silica tube. The produced VCl_2 is retreated by successive heating in vacuum and in HCl gas. By this procedure, most of the higher valence compounds are eliminated. The obtained green flakes of VCl_2 were packed in an aluminium capsule so as to avoid prefered orientation as far as possible. VBr_2 was prepared in the same way as done in VCl_2. VI_2, however, was prepared by direct reaction of vanadium metal and iodine. The equal molar parts of the elements were sealed in a silica tube and slowly heated up to 800°C and kept at this temperature for several days. Then, sublimated small dark violet crystals were obtained. In all the cases, some degree of prefered orientation in the capsule was inevitable.

The diffraction patterns were taken by means of the ISSP ND-1 spectrometer installed at JRR-2, JAERI, Tokai. Most of the patterns were taken using the neutrons of 1.638 Å with a double axis configuration with a soller slit of 30′.

§3. Results

3.1 VCl_2

We first examined the nuclear scattering and confirmed that VCl_2 had CdI_2 structure at He temperature with the parameters listed in Table I. In Fig. 2, a part of the observed diffraction pattern taken at 1.44 K is exhibited. Clearly distinguishable magnetic peaks appear only at 19.4° and 36.4° corresponding to the (1/3 1/3 1/2) and (2/3 2/3 1/2) reflections respectively. The peak at 19.8° is due to the (111)/2 peak for the aluminium capsule. To extract the magnetic part of the intensity more clearly, this aluminium peak evaluated at 77 K is subtracted and the result is shown by the shaded part in the inset with an enlarged scale of ordinate. As can be seen the magnetic scattering consists of two parts. A sharp central peak which might be a conventional Bragg peak and a diffuse scattering which can be seen on both sides. A weak magnetic peak corresponding to the (1/3 1/3 3/2) reflection appears at 30.0° but is diffiuclt to separate clearly from the strong (100) nuclear peak.

Comparison of observed and calculated intensities at very low temperature is given in Table I. In the calculation, we have omitted

Table I. Observed and calculated scattering intensities. 2θ is the scattering angle. The calculated intensities (the corrections for the prefered orientation have been made) for the models in Fig. 3 are given in the last three columns for VCl_2 and VBr_2. The number in the parentheses shows the resultant intensities of the Bragg and diffuse scatterings. All the magnetic reflections marked by M disappear at high temperatures. For VI_2, agreement with the observed angles is good except for the (1 1/2 0)M line which appears at 24.1°. I^{I}_{cal} is the intensity for the model in Fig. 9, whereas I^{II}_{cal} is for the same structure with the moment lying in the c-plane.

(a) VCl_2 $a=3.58_1$ Å $c=5.79_8$ Å $U=0.26$ $T=1.4$ K

Indices	2θ	I_{obs}	I^{I}_{cal}	I^{II}_{cal}	I^{III}_{cal}
001	16.24	1.0	0.53	0.53	0.53
1/3 1/3 1/2 M	19.40	8.8(12.5)	15.7	18.6	14.4
1/3 1/3 3/2 M	30.27	0.6±1.0	4.8	3.3	1.3
100	30.6	37.7	30.4	30.4	30.4
002	32.80	23.6	18.0	18.0	18.0
101	34.8	100.	100.	100.	100.
2/3 2/3 1/2 M	36.4	1.2	2.4	3.4	2.9
102	45.5	20.	23.	23.	23.

(b) VBr_2 $a=3.75_1$ Å $c=6.20_6$ Å $U=0.26$ $T=1.5$ K

Indices	2θ	I_{obs}	I^{I}_{cal}	I^{II}_{cal}	I^{III}_{cal}
001	15.1	0.6	0.7	0.7	0.7
1/3 1/3 1/2 M	18.32	24.6(35.0)	32.3	39.0	30.5
1/3 1/3 3/2 M	28.5	2.8±3.0	10.4	7.4	2.9
100	29.20	37.8	31.5	31.5	31.5
002	30.60	23.	19.	19.	19.
101	33.10	100.	100.	100.	100.
2/3 2/3 1/2 M	34.60	3.9	5.4	7.5	6.5
102	42.82	11.	22.	22.	22.

(c) VI_2 $a=4.02_9$ Å $c=6.71_4$ Å $U=0.26$ $T=4.2$ K

Indices	2θ	I_{obs}	I^{I}_{cal}	I^{II}_{cal}
1/2 0 0 M	13.48	68.	71.	71.
001	14.01	0.	0.8	0.8
1/3 1/3 1/2 M	17.2	22.(at 15.0 K)		
1/2 0 1 M	19.49	40±10.	18.	34.6
1 $\bar{1}$/2 0 M	23.46	13.	18.	0.
1/3 1/3 3/2 M	26.33	—		
100	27.15	33.	32.	32.
1 $\bar{1}$/2 1 M	27.43	10.±10	18.	2.7
002	28.24	23.	20.	20.
101	30.60	100.	100.	100.
0 1/2 2 M	31.42	0.	1.5	7.3
1 1/2 0 M	36.18	11.	8.7	4.9
102	39.58	20.	26.	26.

the Debye-Waller factor. Three magnetic structures (Fig. 3) are tentatively assumed. The first is a model of 120° structure with the moment confined in the basal plane and the intensity is given by I^{I}_{cal} in the table. The second (I^{II}_{cal}) is a model in which the moment lies in the ac-plane keeping the same 120° structure. The last (I^{III}_{cal}) is a model of partially ordered structure, in which two-thirds of spins pointing up and down along the c-axis are ordered forming a honeycomb lattice, while the one-thirds of spins are left paramagnetic. This model can be considered only for the Ising spin systems as appeared in $CsCoCl_3$.[6,7] As the observable magnetic peaks are so few and because of the prefered

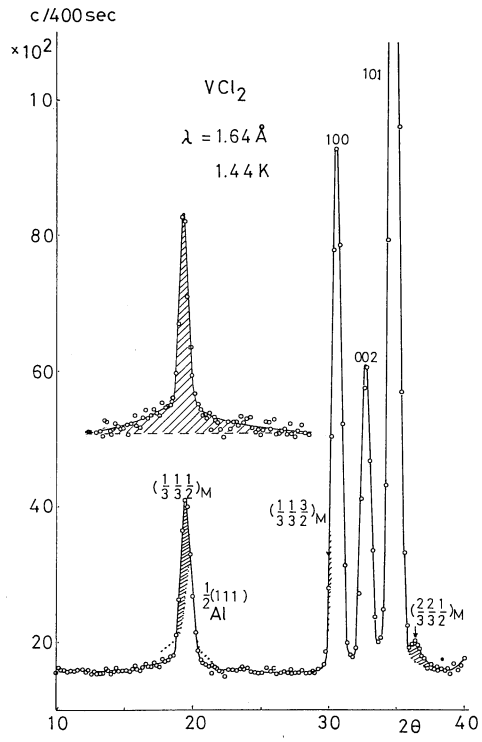

Fig. 2. Diffraction pattern of VCl_2 taken at 1.44 K. The dotted line is the pattern at immediately above T_N showing the strong diffusive tails. To show more clearly the diffuse scattering at 1.44 K, the magnetic part of the scattering is extracted in the inset.

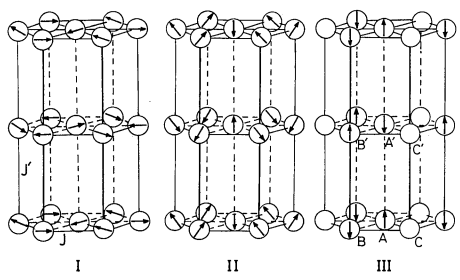

Fig. 3. Three models for the three-sublattice structure. [I] and [II] are the 120° structure and [III] is the partially ordered structure.

orientation effect, the determination of the precise structure is difficult at present. But, unexpectedly, the model III seems most probable though we can not expect strong Ising-like anisotropy in VX_2. The discussion of the structure will be given later.

In Fig. 4 is shown the temperature dependence of the (1/3 1/3 1/2) magnetic peak intensity as appeared in the inset in Fig. 2,

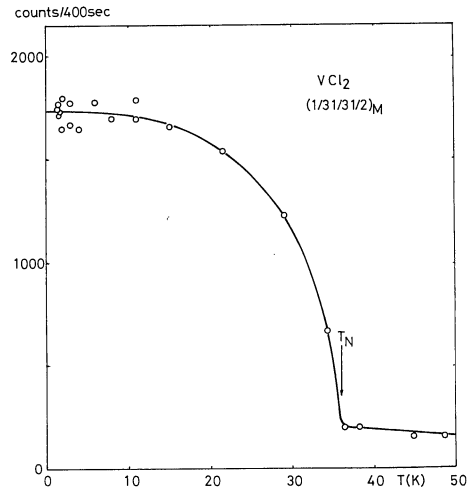

Fig. 4. Temperature dependence of the (1/3 1/3 1/2) magnetic Bragg scattering intensity of VCl_2. The background due to the nuclear incoherent scattering and the Al(111)/2 peak has been subtracted. The counts at $T>T_N$ are due to the SRO.

where all the nonmagnetic background counts have been subtracted. According to the χ-T curve measured by Niel,[3] only a broad maximum around 60 K can be seen. Our neutron scattering pattern shows a well defined T_N at $T_N=36.0\pm0.5$ K but no anomalous behavior could be detected at lower temperatures. In contrast to the conventional case, no rounding of the curve due to the superposition of critical scattering was observed. In other words, the intensity decreases sharply at T_N. On the other hand, as seen in Fig. 4, the intensity at $T\gtrsim T_N$ is still much higher than the background level showing a great contribution of the SRO. The profile of this SRO in the 2θ coordinate can be seen by the dotted line in Fig. 2 taken immediately above T_N. The same features can also be observed in VBr_2 and VI_2 more clearly (refer for instance Fig. 11). This broad SRO peak loses its intensity very gradually with increasing temperature and it vanishes at $\sim 2T_N$. We should note that, contrary to the conventional case, this SRO does not develop asymptotically toward T_N. The profile of the SRO we observe at $T\gtrsim T_N$ has a similar form (width) with the diffuse scattering observed at 1.44 K. So, roughly speaking, the diffuse scattering peak (or SRO peak) change its intensity after

passing through the T_N keeping the profile much the same.

Existence of the strong diffuse scattering at $T \ll T_N$ exhibited in the inset of Fig. 2 is quite unusual. The integrated intensity of the diffuse scattering reaches almost 30% of the total magnatic scattering including both diffuse and Bragg scattering. This is a common property of this VX_2 series and we shall discuss the physical origin later in §4.

3.2 VBr_2

The diffraction pattern of VBr_2 is similar to that of VCl_2. The magnetic peaks are more clearly distinguishable from the nuclear peaks as shown in Fig. 5. The observed intensities at 1.5 K are compared with the calculation in Table I(b). In the present stage, we can not decide which model is the best one. As in the case of VCl_2, the (1/3 1/3 3/2) peak which is estimated after subtraction of the strong (110) nuclear peak is very weak. This weak intensity, though it contains much errors, favor the model III again. But, in VBr_2, this (1/3 1/3 3/2) peak is slightly bigger than for VCl_2 and the other magnetic peaks are less favor for the model III, so that the model I or II may not be ruled out simply. In the present stage, the

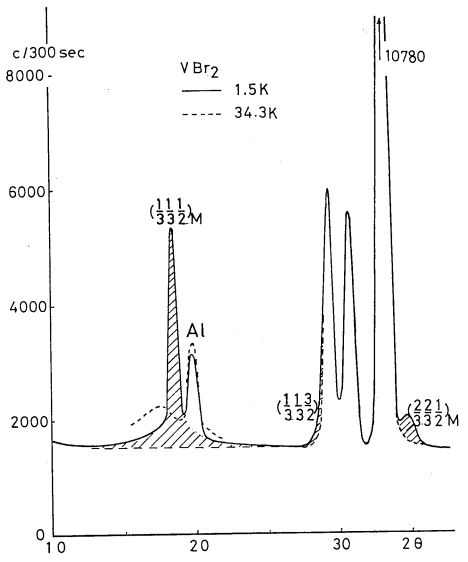

Fig. 5. Diffraction pattern of VBr_2. Note that the magnetic scattering (the shaded part) has broad tails even at 1.5 K around the (1/3 1/3 1/2) peak. The dashed lines are for $T=34.3$ K which is slightly above $T_N=29.5$ K.

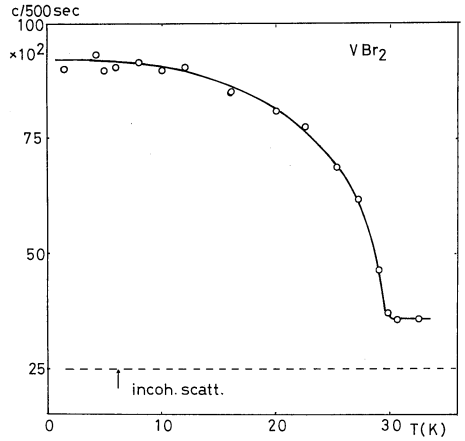

Fig. 6. Temperature dependence of the (1/3 1/3 1/2) magnetic scattering intensity in VBr_2 showing a large residual counts above T_N due to the SRO.

model III is the most probable one. But, with no doubt more precise measurements on the single crystal are desirable.

The temperature dependence of the (1/3 1/3 1/2) magnetic intensity is shown in Fig. 6. The magnetic peak intensity decreases sharply at $T_N=29.5\pm0.5$ K. No rounding of the curve due to the superposition of critical scattering was observed. As in the case of VCl_2, the intensity at $T \gtrsim T_N$ is much higher than the incoherent scattering background showing a great contribution of the SRO. In VBr_2, however, we observed slightly different behavior near the T_N. As shown in Fig. 7, when the scans are made immediately above the T_N, a couple of weak peaks appear at the position $\pm1.2°$ away from the original Bragg position of 18.32°. We have not studied these satellite peaks in detail but they appear suddenly at the same temperature where the main peak vanishes. With increasing temperature, the peak position does not change but the peaks broaden gradually and they can still be recognized at 34.3 K. We suppose that the conical-point instability in the triangular lattice system as proposed by Shiba[8] and observed in $RbFeCl_3$[9] and $CsFeCl_3$[10] may have occured also in VBr_2. It should be noted that even at 1.5 K, still strong diffuse scattering tails are observable as shown by the shaded part in Fig. 5. The integrated diffuse scattering intensity reaches nearly 30% of the total magnetic scattering including both

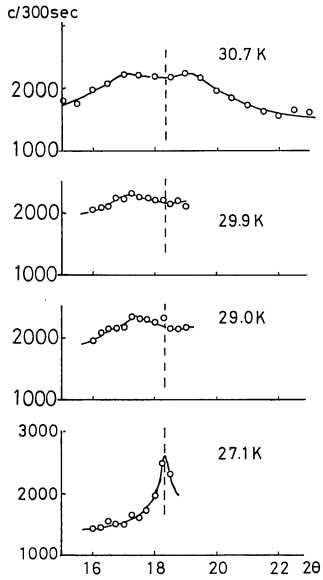

Fig. 7. Details of the 2θ scan at various fixed temperatures near $T_N=29.5$ K in VBr_2 showing appearance of weak satellite peaks at $T \geq T_N$.

diffuse and Bragg scattering. This feature is very similar to the case of VCl_2.

3.3 VI_2

Among VX_2, VI_2 shows different behavior though the crystal and magnetic structures are fundamentally the same. It undergoes a magnetic transition similar to VCl_2 and VBr_2 at $T_{N1}=16.3$ K. But, with further decreasing of temperature, another transition occurs at $T_{N2}=14.4$ K. This transition is of first order. The anomalous behavior in the χ-T curve was first found by Niel *et al.*[3] and somewhat later, Kuindersma *et al.*[11] made a neutron scattering study and determined the magnetic structures on both sides of the T_{N2}. The observed diffraction pattern in their paper is similar to our pattern in the nuclear scattering but the intensities of the magnetic peaks are different. In Fig. 8, our observed diffraction patterns at 77 K ($T>T_{N1}$), 16.0 K (just below T_{N1}) and 8.0 K ($T<T_{N2}$) are reproduced. We have not yet studied the magnetic structure in the phase between T_{N1} and T_{N2} in detail because as the moment is small and more machine time is needed. However, Kuindersma *et al.*[11] have given a structure of the model II in Table I. They have also given a complicatec colliner structure at $T<T_{N2}$. Our observed diffraction pattern is different from their pattern, even the difference of the used wave lengths (consequently the different Lorentz correction) is taken into account. Our magnetic pattern can be explained by a simple model as shown in Fig. 9. This structure is not only different from their result but also different from the structure proposed by Friedt *et al.*[12] from their Mössbauer study. The difference may partly be caused by the difference of the sample. In Table I(c), we have given two model cases to be compared with our observation. The model I is the one shown in Fig. 9, whereas the model II is the same structure with the moments lying in the basal plane. Though the (1/2 0 1) intensity is favorable for the model II, all other magnetic peaks are favorable to the model I, so we think the structure is close to the model I in Table I(c).

In Fig. 10, we exhibit the temperature dependence of the (1/2 0 0) magnetic peak intensity by the open circles. At 4.2 K, the intensity shows almost the saturated value for $S=3/2$ and $g=2.0$ as listed in Table I. No distinguishable diffuse scattering observed in the 3-sublattice phase is observable. But, the background is still somewhat higher than the incoherent scattering level. This seems to be the trace of the diffuse scattering previously seen in the three-sublattice phase though the Bragg peak for this structure can no more be recognized at this temperature. This diffuse scattering tail as can be seen in Fig. 8 ($T<T_{N2}$) is very broad and low in hight.

With increasing temperature, the (1/2 0 0) peak intensity starts to decrease slowly and at 14.4 K it comes down suddenly with a slight tail and it starts to increase slowly passing through a maximum at 25~30 K and then decreases to the background level. This slow increase is due to the increase of the tail associated with the (1/3 1/3 1/2) magnetic SRO. In cooperation with the sudden decrease of the (1/2 0 0) peak at 14.4 K, the (1/3 1/3 1/2) peak appears as shown by the filled circles. In Fig. 11, two scans at selected temperatures are exhibited showing that very strong diffuse scattering appears not only at $T=T_{N1}=16.3$ K (see Fig. 10) but at 18.0 K and 15.0 K as

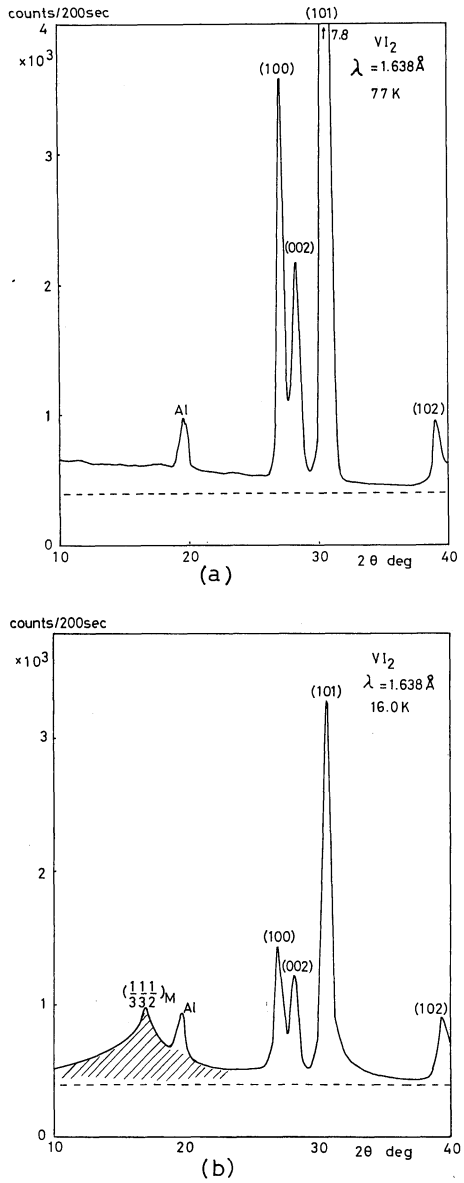

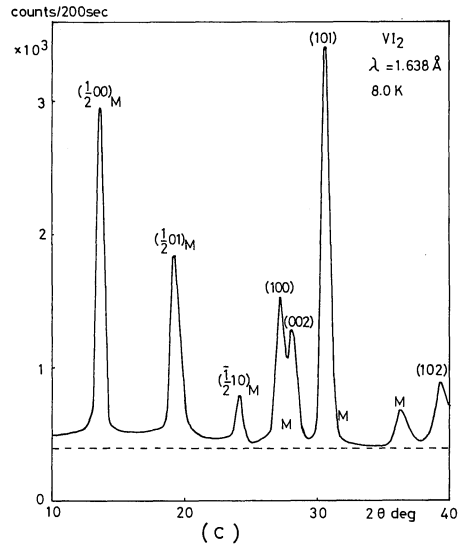

Fig. 8. Powder diffraction patterns of VI_2 taken at 77 K, 16.0 K and 8.0 K. At 77 K no magnetic peaks are observed. At 16.0 K which is just below $T_{N1}=$ 16.3 K a big diffuse scattering is seen around the (1/3 1/3 1/2) magnetic Bragg point. At 8.0 K$<$ $T_{N2}=14.4$ K, new very strong magnetic peaks as marked by M appear. But, very broad background peak centred around 18° can still be seen. Note that the (1/2 0 1)M peak contains Al (111)/2 peak.

well. We think that this diffuse peak which appears over a very wide range of temperature is one of the most remarkable properties in the frustrated system. We should note that this diffuse peak is symmetric on both sides. At sufficiently high temperature such as 77 K, the diffuse scattering vanishes leaving a typical feature of paramagnetic scattering as seen in Fig. 8(a).

§4. Discussion

We have studied powder diffraction patterns of VX_2 which are thought to represent characters of quasi-2D triangular, $S=1/2$ Heisenberg antiferromagnets. In VX_2 with CdI_2 structure, the cation sheets are separated by the two-interpenetrating anion sheets forming a layer structure. Consequently, one would expect a 2D character of magnetic interactions though it should be checked by the inelastic scattering study. In fact, the large Weiss constants suggest very strong negative interactions within the layers. As it is difficult to imagine such a strong coupling to exist between the layers, the system will behave 2D-like though not perfectly. Un-

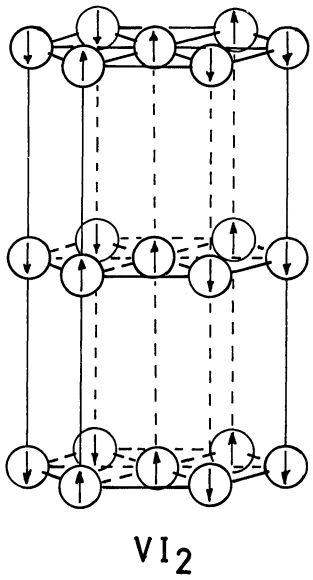

Fig. 9. The proposed plausible magnetic structure of VI_2 in the low temperature phase.

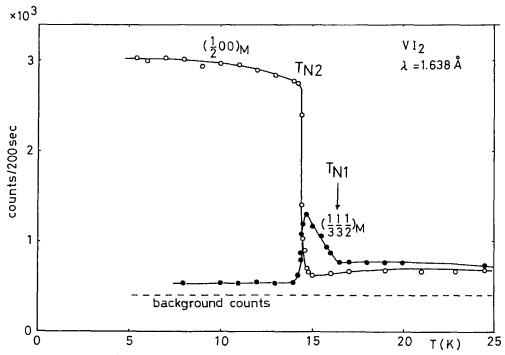

Fig. 10. Temperature dependence of the scattering intensity at $2\theta=13.48°$ where the (1/2 0 0)M peak is observable at $T<T_{N2}$, (shown by ○). The intensity at $2\theta=17.2°$ where the (1/3 1/3 1/2)M appears at $T>T_{N2}$ is shown by the ●. A strong SRO can be seen at $T>T_{N1}$ over a wide range of temperature.

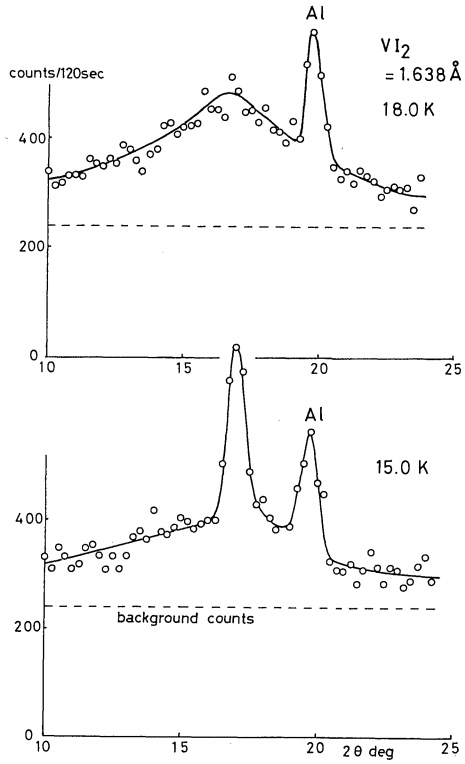

Fig. 11. Typical scans to see the diffuse scattering, one at $T>T_{N1}$ and another at $T<T_{N1}$ in VI_2. The line shape of the diffuse scattering is not very much changed but the intensity decreases at 15 K to the extent by which the Bragg peak intensity increased. Note that the pattern appeared at 18 K persists well above the T_{N1}.

expectedly, however, as far as our quasi-elastic scattering patterns are concerned, no SRO characteristic for 2D can be seen. If the system is ideally 2D and if the SRO associated with the 3-sublattice structure is developed in the 2D plane, one would observe asymmetric diffuse scattering being steep on the lower angles and gentle on the higher angles. In any case of VX_2, the diffuse (SRO) pattern is nearly symmetric. We suppose that the development of the correlation length of antiparallel configuration in the 2D-plane is greatly suppressed in such a triangular lattice antiferromagnet by the partial cancellation of the intraplane Weiss fields. Thus, the interactions which are not responsible for the frustration, such as interplane coupling, makes a greater role for the appearance of the LRO. This may make the transition more likely to be of 3D. Throughout this study, we have two problems to be discussed. One is the problem that what is the most probable spin structure observed below the transition. Another is the question that what is the origin of the strong diffuse scattering observed at $T>T_N$ and the one observed even at very low temperatures $T\ll T_N$ and the relation between these two diffuse scatterings.

4.1 The spin structure below T_N ··· mainly on VCl_2 and VBr_2

It is not easy to determine the spin structure based on a few limited number of magnetic reflections. But the fact that (*hkl*) magnetic peak appears when $h=k=1/3,\ 2/3,\ 4/3\cdots$ etc. and $l=n+1/2$ suggests six-sublattice structures as shown in Fig. 3. In these structures, one basal plane is composed of three sublattices A, B and C and each of them forming two-sublattice structure AA′, BB′ and CC′ along the *c*-axis. As for the orientation of spins, we have no foresight of prefered axis, because, after the ESR study by Yamada and Hirakawa,[13] $g_a=1.994$ and $g_c=1.992$ for VBr_2 suggesting very small anisotropy energy if any compared to the exchange energy. Therefore, the spin systems are very well approximated by the Heisenberg model. As the exchange energy in the classical Heisenberg system in the triangular lattice antiferromagnet is best stabilized by forming the 120° structure, we calculated the scattering intensity for the two different orientations but with the same structure as in Fig. 3 (mode I and II). According to Shiba,[14] the dipole-dipole interaction favour the model [II] rather than [I] but the energy difference is very small. As stated before, however, neither [I] nor [II] can explain the observed results as seen in Table I. Disagreements are in that the observed magnetic intensities especially for the (1/3 1/3 3/2) reflection at $T\ll T_N$ are too weak compared to the calculated one. In order to avoid this difficulty, we have calculated the third model [III], in which the A and the B sublattices make an collinear spin alignment on the honeycomb lattice leaving the C sublattice paramagnetic as shown in Fig. 3. This structure has already been found in $CsCoCl_3$ in which the Ising-like antiferromagnetic chains along the *c*-axis are coupled antiferromagnetically in the basal plane.[6,7] This model is easily accepted intuitively in the Ising system but it is hard to be accepted in the Heisenberg system. Surprizingly, however, our observed magnetic peaks are rather close to this partially ordered model. Even for this model, the observed Bragg scattering intensities are still considerably lower than the calculation. It is interesting, however, that in the (1/3 1/3 1/2) peak if the sum of the Bragg part and the diffusive part is taken as the (1/3 1/3 1/2) intensity, the agreement becomes satisfactory. This suggests that the diffuse scattering at $T\ll T_N$ is caused by the fluctuation of spins within the A and B sublatices. The realization of the model [III[is not so simply ruled out at finite temperature because the exchange energy for models [I] and [II] is only 1.5 times lower than for the model [III] whereas the model [III] has more entropy because the *c*-sublattice can be chosen at any site of the three. Our experiments, however, has been made at sufficiently low temperatures so that the preference of the model [III] rather than [I] or [II] is still left as a question. A quantum effect may be a possible origin. Three sublattices tentatively considered above are not necessarily frozen at their own positions but interchangable. If the frequency of interchange is not so rapid as to allow for the static approximation on the scattering process of neutrons, we would observe an instantaneous pattern as given by the model [III]. Recent NMR observation of extremely small magnetic moment in VCl_2 and VBr_2 ($\sim 30\%$ of the full moment) by Yasuoka *et al.*[15] is indicative of the dynamical fluctuation faster than the NMR frequency.

In Fig. 12, the temperature dependence of sublattice magnetization $M_s(T)$ in VCl_2 and VBr_2 as shown in Figs. 4 and 6 is reproduced by the reduced scales. Both curves for VCl_2 and VBr_2 are in good agreement and they are shown by the single dashed line. In the same figure, the curves for the other two 2D spin systems in which the spin wave approximation is well applicable are shown together. It should be noted that the initial slope of $M_s(T)$ for VX_2 at the lowest temperatures is very flat like Ising system compared with the other two. This means that $M_s(T)$ curve behaves as if there is an energy gap in the excitation spectrum. It is quite unusual that in such a soft anisotropy system the magnetization behaves like Ising system. One of the explanation for this is as follow. If the model III is correct at low temperature, when the paramagnetic C sublattice is ignored, the honeycomb lattice would have very high T_N of the order of the Weiss constant mentioned in §1, thus

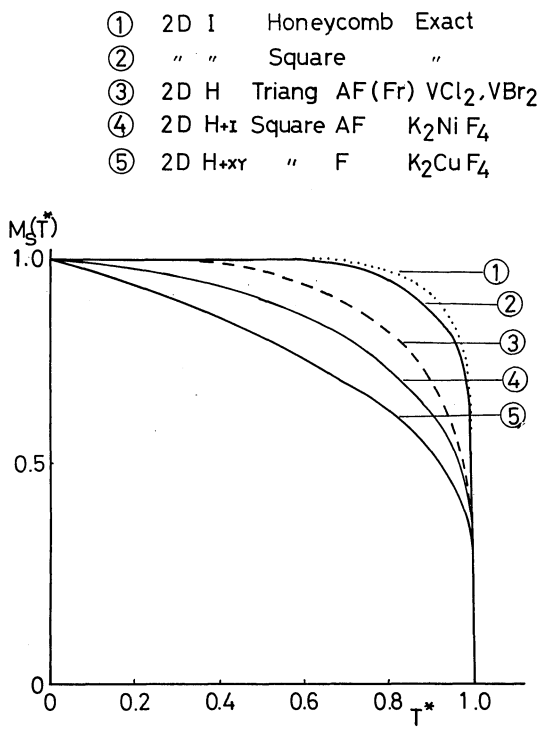

Fig. 12. Normalized temperature dependence of the spontaneous magnetization curve in VCl_2 and VBr_2 derived from Figs. 4 and 5 as compared with the proto-type 2D Heisenberg-like magnets and the 2D Ising systems.

the temperature variation of $M_s(T)$ at lowest temperature is very slow. With elevating temperature however, the interchange among three sublattices becomes more frequent and the $M_s(T)$ will be destroyed more rapidly to produce T_N.

4.2 Diffuse scattering

In the conventional non-frustrated system, the critical scattering occurs centered at the point where the Fourier component $|J(Q)|$ has a maximum value. When the temperature is decreased from above toward T_N, the correlation length increases, i.e. the width of the diffuse (SRO) peak reduces and the maximum intensity increases asymptotically with certain critical indices. The diffuse scattering in the present case is quite different. It does not change its width appreciably and its intensity as well. The temperature change occurs very gradually and does not show a clear asymptotic behavior toward T_N. With approaching T_N, the intensity increases gradually and the width tends to narrow but the change is little as more clearly seen in Figs. 10 and 11. On passing through T_N, the intensity is reduced quickly keeping the shape unchanged. Even at very low temperatures, it can still be observed with considerable intensity. The width at these temperatures corresponds to the correlation length of 2~3 atomic distances in the plane. One possible explanation is that some impurities most probably of the V^{3+} ions cause local distortions of the spin orientation extending over considerable range of neighbours. According to the susceptibility measurements,[16] the possible impurity is less than 0.5%, so that this will not be the case, though may not be ruled out simply. Stacking fault of the crystal structure may also be considered but the nuclear diffuse scattering is not so strong as to account for this. Another explanation is that the spins in the plane are not fixed in a fixed direction but interchangeable with a certain rate. Especially in the model [III], the spins can exchange their directions among the neighbours through the off-diagonal term. So that the spins are fluctuating locally but keeping the A and B sublattice structure as a whole. This local fluctuation which might be a zero point motion is quicker than the frequency of the sublattice interchange stated before. This local fluctuation will cause the reduction (~30%) of the A and B sublattice moment mentioned in 4.1 and the diffuse scattering. This model of partial order seems to be a bold argument, but seems to explain many misterious properties hitherto observed. The idea is in a sense similar to Anderson's movable valence bond picture[16] as mentioned in the introduction.

Hitherto, we have not mentioned much about VI_2 but the behavior at temperatures higher than T_{N2} is very similar to the cases of VCl_2 and VBr_2. As we have grown the single crystal, detailed study will be reported shortly. As for the structure below T_{N2}, it seems sensitive to the condition of the preparation of the sample. But, it has a collinear structure at $T<T_{N2}$ and no anomalous behavior as mentioned above has been observed and a full moment can be observed. This means that

the above mentioned spin contraction is not due to the covalency effect. We are not involved in the precise determination of the structure at present.

As a conclusion, we have an impression that the ground state of VX_2 may not be the Néel structure in which the spins make an angle of 120° with each other but is a partially ordered structure in which A and B sublattices are ordered collinearly antiferromagnetically forming a honeycomb lattice leaving the C sublattice paramagnetic. In this model spins are locally interchanging their directions rapidly but changing the sublattice much more slowly.

Recent ESR experiments by Yamada *et al.*[13] is indicative of realization of this model. The ESR signal appeared in the paramagnetic phase of VBr_2 disappears at T_N with lowering temperature but reappears at $T<T_N$. Complete diminishing of the anisotropy in the single crystal susceptibility in VCl_2, VBr_2 and VI_2 in the three sublattice phase as measured by SQUID magnetometer[17] is also striking. The NMR signal studied by Yasuoka and Tsuda[15] is quite unusual. Not only the reduction of the moment but the NMR spectra under the external field at $T<T_N$ does not change when the direction of field is changed showing as if the spins in the ordered phase does not have a fixed direction. The enhancement effect of the NMR signal is comparable to the case of ferromagnet though the static susceptibility is very small. These misterious properties indicates as if the spins at $T<T_N$ behaves like a magnetic (quantum ?) fluid, and the nature of the transition may completely be different from the conventional one.

Finally, we suppose, through this study that the big spin contraction in $CsVCl_3$ is caused mainly through its excellent 1D nature with zero point motion of spins, but some parts of the spin contraction are caused by the same mechanism as mentioned in this section on VX_2. In fact some amount of diffuse scattering can also be observed at very low temperature in $CsVCl_3$.

We are grateful to Professor H. Shiba and Dr. S. Miyashita for valuable discussions. Invaluable NMR information from Professor H. Yasuoka, ESR data from Professor I. Yamada, cooperation of susceptibility measurement by Professor H. Ikeda and technical help by Mr. Y. Kawamura at JAERI, Tokai are greatly acknowledged. This work was performed at JRR-2, JAERI, Tokai.

References

1) P. Fazekas and P.W. Anderson: Philos. Mag. **30** (1974) 423.
2) H. Yoshizawa, K. Ubukoshi and K. Hirakawa: J. Phys. Soc. Jpn. **48** (1980) 42.
3) M. Niel, C. Cros, G. Le Flem, M. Pouchard and P. Hagenmuller: Physics **86–88B** (1977) 702; M. Niel: Thesis, L. Univ. de Bordeaux 1976.
4) K. Hirakawa, H. Yoshizawa and K. Ubukoshi: J. Phys. Soc. Jpn. **51** (1982) 1119.
5) H. Kadowaki, K. Hirakawa and K. Ubukoshi: to J. Phys. Soc. Jpn. **52** (1983) 1799.
6) M. Mekata: J. Phys. Soc. Jpn. **42** (1977) 76.
7) H. Yoshizawa and K. Hirakawa: J. Phys. Soc. Jpn. **46** (1979) 448.
8) H. Shiba: Solid State Commun. **41** (1982) 511. H. Shiba and N. Suzuki: J. Phys. Soc. Jpn. **51** (1982) 3488.
9) N. Wada, K. Ubukoshi and K. Hirakawa: J. Phys. Soc. Jpn. **51** (1982) 2833.
10) W. Knop, M. Steiner and P. Day: *Int. Conf. Mag. Kyoto* (1982).
11) S. K. Kuindersma, C. Haas, J. P. Sanchez and R. Al: Solid State Commun. **30** (1979) 403.
12) J. M. Friedt, J. P. Sanches and G. K. Shenoy: J. Chem. Phys. **65** (1976) 5093.
13) I. Yamada and K. Hirakawa: in preparation.
14) H. Shiba: private communications.
15) H. Yasuoka and T. Tsuda: in preparation.
16) P. W. Anderson: Mat. Res. Bull. **8** (1974) 423.
17) K. Hirakawa, H. Ikeda, H. Kadowaki and K. Ubukoshi: submitted to J. Phys. Soc. Jpn.